Journal of Experimental Botany, Vol. 73, No. 19 pp. 6902–6915, 2022
https://doi.org/10.1093/jxb/erac308 Advance Access Publication 11 July 2022

RESEARCH PAPER

A *Phytophthora* effector promotes homodimerization of host transcription factor StKNOX3 to enhance susceptibility

Jing Zhou[1,2,3,4], Yetong Qi[1,2,3], Jiahui Nie[1,2,3], Lei Guo[5], Ming Luo[1,2,3], Hazel McLellan[6], Petra C. Boevink[7], Paul R. J. Birch[6,7] and Zhendong Tian[1,2,3,4,*],

[1] Key Laboratory of Horticultural Plant Biology (HZAU), Ministry of Education, Huazhong Agricultural University (HZAU), Wuhan, Hubei, 430070, China
[2] Key Laboratory of Potato Biology and Biotechnology (HZAU), Ministry of Agriculture and Rural Affairs, Wuhan, China
[3] Potato Engineering and Technology Research Center of Hubei Province (HZAU), Wuhan, China
[4] Hubei Hongshan Laboratory (HZAU), Hubei Province, Wuhan, China
[5] College of Agronomy, Northeast Agricultural University, Harbin, 150030, China
[6] Division of Plant Sciences, University of Dundee, At James Hutton Institute, Errol Rd, Invergowrie, Dundee DD2 5DA, UK
[7] Cell and Molecular Sciences, James Hutton Institute, Errol Road, Invergowrie, Dundee DD2 5DA, UK

* Correspondence: tianzhd@mail.hzau.edu.cn

Received 24 January 2022; Editorial decision 6 July 2022; Accepted 11 July 2022

Editor: Monica Höfte, University of Ghent, Belgium

Abstract

Oomycete pathogens secrete hundreds of cytoplasmic RxLR effectors to modulate host immunity by targeting diverse plant proteins. Revealing how effectors manipulate host proteins is pivotal to understanding infection processes and to developing new strategies to control plant disease. Here we show that the *Phytophthora infestans* RxLR effector Pi22798 interacts in the nucleus with a potato class II knotted-like homeobox (KNOX) transcription factor, StKNOX3. Silencing the ortholog *NbKNOX3* in *Nicotiana benthamiana* reduces host colonization by *P. infestans*, whereas transient and stable overexpression of *StKNOX3* enhances infection. StKNOX3 forms a homodimer which is dependent on its KNOX II domain. The KNOX II domain is also essential for Pi22798 interaction and for StKNOX3 to enhance *P. infestans* colonization, indicating that StKNOX3 homodimerization contributes to susceptibility. However, critically, the effector Pi22798 promotes StKNOX3 homodimerization, rather than heterodimerization to another KNOX transcription factor StKNOX7. These results demonstrate that the oomycete effector Pi22798 increases pathogenicity by promoting homodimerization specifically of StKNOX3 to enhance susceptibility.

Keywords: Class II knotted-like homeobox (KNOX) transcription factor, effector, homodimerization, pathogenicity, plant immunity, potato late blight.

Introduction

Plants are exposed to attack by a wide variety of pathogens. In order to protect themselves, plants have evolved two layers of immunity (Jones and Dangl, 2006). Plants can recognize conserved pathogen/microbe-associated molecular patterns (P/MAMPs) to activate the primary immune system, pattern-triggered immunity (PTI) (Dodds and Rathjen, 2010). The

proteins that recognize P/MAMPs are named pattern recognition receptors (PRRs) (Brunner *et al.*, 2002; Zipfel et al., 2004, 2006; Chinchilla *et al.* 2006). However, pathogens secrete small proteins called effectors that can act either inside (cytoplasmic) or outside (apoplastic) the host cell to suppress PTI. A number of host proteins targeted by cytoplasmic effectors from filamentous (fungal and oomycete) pathogens have been identified, revealing the manipulation of diverse processes such as protein regulation, signaling, metabolism, cellular trafficking, transcription, and RNA processing (Wang *et al.*, 2019a; He *et al.*, 2020). To overcome the action of effectors, a second layer of the immune system is initiated. Some effectors are recognized by conserved nucleotide-binding leucine-rich repeat (NLR) proteins, directly or indirectly, resulting in effector-triggered immunity (ETI) (Jones and Dangl, 2006; Dodds and Rathjen, 2010).

Late blight remains the most devastating disease of potato, threatening its production and quality (Fry *et al.*, 2015; Kamoun *et al.*, 2015). The late blight pathogen *Phytophthora infestans* delivers multiple functional effectors into the plant cell to manipulate immunity. Those delivered into the cell include RxLR effectors, so named as they contain a conserved motif, Arg–X–Leu–Arg, where X is any amino acid (Haas *et al.*, 2009; Win *et al.*, 2012). After secretion from haustoria and translocation into plant cells, effectors target one or more host proteins to promote infection (Whisson *et al.*, 2016; S. Wang *et al.*, 2017, 2018). The first reported RxLR effector target in potato is the ubiquitin E3 ligase CMPG1 (Bos *et al.*, 2010). The interacting effector Avr3a stabilizes CMPG1 to benefit the pathogen. Since then, numerous *P. infestans* effectors and their targets have been identified, revealing a diversity of processes that are manipulated. For example, effector Pi04089 interacts with RNA-binding protein StKRBP1 to promote infection (Wang *et al.*, 2015); Pi04314 targets PP1c isoforms to enhance pathogen colonization through manipulating their phosphatase activity (Boevink *et al.*, 2016); Pi02860 interacts with the E3 ligase StNRL1 which degrades a positive immune regulator StSWAP70 to suppress PTI (Yang *et al.*, 2016; He *et al.*, 2018); PexRD2 and Pi22926 target different mitogen-activated protein kinase (MAPK) pathway components and both suppress the hypersensitive response (HR) induced by Cf4/Avr4 (King *et al.*, 2014; Ren *et al.*, 2019); Pi03192 prevents the immune-associated re-localization of two NAC transcription factors (TFs; McLellan *et al.*, 2013); and Pi20303 and Pi20300 stabilize the potato MAPK cascade signaling protein MKK1 to negatively regulate the plant PTI response (Du *et al.*, 2021). Many of these examples show that *P. infestans* RXLR effectors interfere with host immunity at different steps and in different locations to promote virulence (Wang *et al.*, 2019a; He *et al.*, 2020).

Plant-specific *KNOTTED1-LIKE HOMEOBOX* (*KNOX*) genes belong to the Three Amino Acid Loop Extension (TALE) homeodomain superfamily (Bertolino *et al.*, 1995; Hay and Tsiantis, 2010). *KNOX* genes are divided into two classes: *KNOX I* and *KNOX II*, based on their sequence similarity, expression pattern, and functions (Kerstetter *et al.*, 1994). The class I *KNOX* genes, which are evolutionarily close to the first plant *KNOX* gene *KNOTTED1* identified from maize (Vollbrecht *et al.*, 1991), are predominantly expressed in the shoot apical meristem (SAM) and play critically important roles in SAM development, diversity, and leaf morphology (Sinha *et al.*, 1993; Dockx *et al.*, 1995; Long *et al.*, 1996; Byrne *et al.*, 2002; Douglas *et al.*, 2002; Belles-Boix *et al.*, 2006; Ragni *et al.*, 2008; Shani *et al.*, 2009). The expression pattern of class II *KNOX* genes is more uniform, being detected in almost all plant tissues.

In Arabidopsis, the class II *KNOX* genes are divided into two subclasses: *KNAT7* and *KNAT3/4/5* (Mukherjee *et al.*, 2009). Compared with class I *KNOX* genes, less is known about the diverse functions of class II *KNOX* genes. In Arabidopsis and rice, KNAT7 is involved in the regulation of secondary cell wall development and cell growth through different protein interactions and gene regulatory pathways (Brown *et al.*, 2005; Ehlting *et al.*, 2005; Persson *et al.*, 2005; Zhong *et al.*, 2008; Bhargava *et al.*, 2013; Liu *et al.*, 2014; Huang *et al.*, 2015; Liu and Douglas, 2015; Wang *et al.*, 2019b; Yu, 2019). In *Medicago truncatula*, KNAT3/4/5 encode four highly homologous proteins with functional redundancy, which may regulate the development of legume symbiotic nodules and control the boundary and shape of nodule organs potentially through the MtEFD/MtRR4 cytokinin-related regulatory module (Di Giacomo *et al.*, 2017). Meanwhile, MtKNOX3 can directly bind the promoters of *MtLOG1*, *MtLOG2*, and *MtITP3* to regulate symbiotic nodule development (Azarakhsh *et al.*, 2015, 2020). In rice, KNAT3 interacts with another TALE TF—BLH1—and participates in embryo sac development (Pagnussat *et al.*, 2007), flowering (Smaczniak *et al.*, 2012), abscisic acid (ABA)-induced seed germination, and early development (Hackbusch *et al.*, 2005; D. Kim *et al.*, 2013). Recent studies have found that KNAT3 can heterodimerize with KNAT7 to synergistically regulate the biosynthesis of monoalcohols, thus promoting the biosynthesis of the secondary cell wall (Qin *et al.*, 2020; Wang *et al.*, 2020), while concurrently acting antagonistically with KNAT7 to inhibit the formation of secondary cell wall intercellular fibers (Wang *et al.*, 2020).

Our previous research identified a conserved *P. infestans* RxLR effector Pi22798 that is induced early during infection and promotes pathogen colonization. In addition, Pi22798 contains a C-terminal nuclear localization signal (NLS), and its virulence activity requires its nuclear localization (H. Wang *et al.*, 2017). In this study, a potential target of Pi22798 was identified by screening a potato–*P. infestans* interaction yeast two-hybrid (Y2H) library (Bos *et al.*, 2010). The interacting protein, StKNOX3, the candidate ortholog of KNAT3 from Arabidopsis, belongs to the class II KNOX TF family. Expression of *StKNOX3* in *Nicotiana benthamiana* enhanced infection, indicating that StKNOX3 may act as a negative regulator of defense against *P. infestans*. StKNOX3

homodimerization is required to enhance pathogen colonization, and its KNOX II domain is essential for dimerization, for Pi22798 interaction, and for it to promote susceptibility. Finally, co-immunoprecipitation (Co-IP) and spilt-luciferase (LUC) assays demonstrate that Pi22798 promotes the homodimerization of StKNOX3. Our results suggest that the oomycete effector Pi22798 increases pathogenicity by promoting homodimerization of the host TF StKNOX3.

Materials and methods

Plasmid constructs

Specific primers with flanking attB sites for *PITG_22798* (XP_002998395.1) and *StKNOX3* (NP_001305543.1) were used to amplify genes from *P. infestans* DNA or potato cDNA by PCR. Primer sequences are shown in Supplementary Table S1. After purification, the PCR products were recombined into entry vector pDONR221 (Invitrogen, Carlsbad, CA, USA) through BP reaction. Then the entry clones were recombined into destination vectors, which include pDEST32/22 (for Y2H assay; Invitrogen), pB7WGF2.0 [for N-terminal enhanced green fluorescent protein (eGFP) fusion], pK7WGR2.0 [for N-terminal red fluorescent protein (RFP) fusion], and PCL112/113 (for bimolecular fluorescence complementation (BiFC)]. The deletion mutants of StKNOX3 were obtained by recombination of two separate parts and cloned as above.

For HA-tagged Pi22798, PiSFI3, and Pi04089, the effectors were amplified with gene-specific primers containing the *Stu*I restriction site and constructed into the pH7C-LIC7.0-3×HA vector. For both Myc- and monomeric RFP (mRFP)-tagged StKNOX3, mRFP and StKNOX3 were amplified from pJCV55 vector and potato cDNA, respectively. Purified PCR products were recombined into a single sequence using ClonExpress II One Step Cloning Kit (Vazyme Biotech Co., Ltd, Nanjing, China). Then the double-tagged StKNOX3 clones were obtained as above.

All the constructs used in this study are listed in Supplementary Table S1.

Agroinfiltration and P. infestans infection assay

Agrobacterium tumefaciens GV3101-containing expression vectors were cultured overnight in yeast extract and beef (YEB) medium, then centrifuged and resuspended in MMA buffer (10 mM MES, 10 mM $MgCl_2$, and 200 mM acetosyringone). Before infiltration, the bacteria were adjusted to the appropriate OD_{600} (0.5 for western blot and Co-IP; 0.1 for infection assay; 0.001 for image capture).

Phytophthora infestans isolate 88069 was used to infect *N. benthamiana* and potato. After growth in rye agar for 2–3 weeks, the sporangia were collected from plates and suspended in the required ddH_2O volume. The final sporangial number was adjusted to ~100 μl^{-1} and the inoculum was stored at 4 °C for 2–4 h. Droplets of 10 µl were inoculated on *N. benthamiana* or potato leaves 1 d after agro-infiltration. Lesion sizes were measured 4–7 dpi (days post-inoculation).

Plant materials

Nicotiana benthamiana plants were grown in a growth chamber in 16 h days at 22 °C, and potato (*Solanum tuberosum*) plants were grown in a greenhouse under natural conditions; 3- to 4-week-old *N. benthamiana* and 7- to 8-week-old potatoes were used for experiments.

Genetic modification of potato

Agrobacterium tumefaciens LBA4404-containing vector expressing Myc-StKNOX3–mRFP was transformed into potato cultivar 'Désirée' by leaf disc transformation according to Zhan *et al.* (2019). The positive lines were selected in Murashige and Skoog (MS) medium containing 100 mg l^{-1} kanamycin and confirmed by PCR using the promoter p35S and a gene-specific reverse primer. Gene expression levels were analyzed by quantitative reverse transcription–PCR (RT–qPCR) using both *StActin* and *StTUB* as reference genes (primers are shown in Supplementary Table S1).

Genetic modification of N. benthamiana

Leaf discs were used for transformation utilizing *A. tumefaciens* containing the overexpression vector GFP–StKNOX3. The transformation procedures and seed collection were according to Wang *et al.* (2018).

Gene expression assay

For gene expression assay, the RNA was extracted using a total RNA purification kit (Aidlab Biotechnologies Co., Ltd, Beijing China) and revers transcripted into cDNA. Quantitative real-time PCR (qRT-PCR) was performed using Evergreen Express 2×qPCR MasterMix (abm®, Applied Biological Materials Inc., Guangzhou, China) on a Bio-Rad PCR machine. The PCR conditions are 95 °C for 3 min, followed by 40 cycles (95 °C for 5 s, 58 °C for 15 s). Data were analyzed by the $2^{-\Delta\Delta CT}$ method (Livak and Schmittgen, 2001), with expression normalized to the housekeeping genes. Primers used in this study (Supplementary Table S1) were designed at the Primer-BLAST of NCBI website, and primer quality was tested by melting curve.

Virus-induced gene silencing (VIGS) in N. benthamiana

Approximately 300 bp fragments from the 3′-untranslated region (UTR) of *NbKNOX3* was constructed into pBinary *Tobacco rattle virus* (TRV2) vectors (Fu *et al.*, 2005) between the *Eco*RI and *Bam*HI restriction sites in the antisense orientation. Primer sequences are shown in Supplementary Table S1. A TRV2 vector expressing a fragment of GFP was used as control. *Agrobacterium tumefaciens* GV3101 containing plasmids were incubated in YEB medium overnight and resuspended in infiltration buffer. The final OD_{600} of each bacterium was adjusted to 0.3, then mixed with the TRV1 vector in the same volume. Four-leaf stage *N. benthamiana* were used for VIGS. Silencing efficiency was tested by gene-specific primers using the *N. benthamiana* housekeeping gene *Actin* as a control because of its abundance and consistency of Ct values among tissues and treatments. The two largest leaves were fully infiltrated and the plants were grown in 22 °C under suitable humidity and used 2–3 weeks after virus infection for infection assay.

Y2H assay

We used the ProQuest system (Invitrogen) for screening of the Y2H library. The potato yeast library and the screening methods are as previously reported (Bos *et al.*, 2010). Effector Pi22798 was cloned into the 'bait' vector pDest32 by the gateway cloning method. The targeted plasmid was transformed into yeast stain MAV203 according to the manual (Invitrogen, PQ10001-01 and PQ10002-01). The positive clones were selected in medium lacking histidine (SD-Leu-Trp-His) and confirmed by regrowth in SD-Leu-Trp-His medium and gain of β-galactosidase (X-gal) activity.

Western blot and immunoprecipitation

Agrobacteria containing the relevant plastids were co-expressed in *N. benthamiana* leaves. Two days after infiltration, the leaf tissues were sampled and frozen in liquid nitrogen. For western blot, samples were milled and mixed with 200 µl of protein extraction buffer {GTEN buffer [10%

(v/v) glycerol, 25 mM Tris–HCl (pH 7.5), 1 mM EDTA, 150 mM NaCl] with 10 mM DTT, protease inhibitor cocktail (Roche Life Science), 1 mM phenylmethyl sulfonylfluoride (PMSF), and 0.2% NP-40}. After a 30 min incubation in ice, the samples were centrifuged at 4 °C for 10 min and supernatants were removed and mixed with 2× SDS sample buffer, and boiled at 95 °C for 10 min. Proteins were separated on 8–12% SDS–PAGE gels and transferred to polyvinylidene fluoride (PVDF) membranes. After incubation with primary antibody [anti-GFP and anti-Myc from Sungene (Tianjin Sungene Biotech Co., Ltd) and anti-HA and secondary antibody from MBL (MBL Beijing Biotech Co., Ltd, Beijing, China)], the membranes were visualized using chemiluminescent ECL (Servicebio, Wuhan, China).

For GFP-tagged Co-IP, the samples were milled and mixed with 500 µl of protein extraction buffer. The extraction supernatants were separated into two parts. A 50 µl aliquot of the supernatant was added to 2× SDS sample buffer and boiled at 95 °C for 10 min, and the rest was added to 20 µl of GFP-Trap_M beads (MBL) or GFP agarose beads (AlpaLife), incubated at 4 °C for 2 h. Beads were washed with 500 µl of wash buffer (GTEN with protease inhibitor cocktail and 1 mM PMSF) three times and resuspended in 2× SDS sample buffer. Samples were then processed by western blot as above.

Split luciferase complementation assay

The spilt-LUC vector pCAMBIA-1300 was used for construction of carriers between the *Eco*RI and *Bam*HI restriction sites, and nLUC/cLUC are the empty vectors. Primer sequences are shown in Supplementary Table S1. Two days after infiltration, the infiltrated sites were sprayed with 100 mM D-luciferin and kept in the dark for 15 min. The fluorescence was detected and analyzed using bioluminescence imaging with indiGO software. The stability of spilt-LUC constructs was detected by western blot using anti-luciferase antibody (Sigma, Cat. No. L0159).

Live cell imaging

Two-day-infiltrated leaves of *N. benthamiana* expressing the targeted proteins were prepared for imaging in a Leica LCS confocal microscope. GFP fluorescence was excited with 488 nm from an argon laser and its emissions were detected between 500 nm and 530 nm. RFP fluorescence was excited with 561 nm and its emissions were collected between 600 nm and 630 nm. Sprite yellow fluorescent protein (YFP) was excited using 514 nm from an argon laser with emissions detected from 530 nm to 575 nm. Images were collected from leaf cells expressing relatively low levels of the protein fusions to minimize possible artifacts of ectopic protein expression. Images were quantified using the ImageJ and Leica LCS software packages as required.

Results

Pi22798 interacts with the potato homeodomain transcription factor KNOX3

To identify candidate targets of *P. infestans* effector Pi22798 in its host, potato, a Y2H library made from *P. infestans*-infected potato leaves (Bos *et al.*, 2010) was screened with a GAL4-binding domain–Pi22798 fusion construct (bait). After two rounds of independent screening, two yeast colonies were recovered from selection plates containing GAL4 activation domain (prey) fusion sequences corresponding to potato transcript PGSC0003DMT400078989 (annotated as homeobox protein knotted-1-like LET12). This gene encodes a protein containing a homeobox domain and is a reciprocal best blast hit of the *Arabidopsis thaliana* KNOX II clade member AtKNAT3 (AT5G25220.1). It is hereafter called StKNOX3 (KNOTTED-LIKE HOMEOBOX 3). StKNOX3 shares high identity with homeobox proteins possessing conserved KNOX I, KNOX II, ELK, and homeobox domains (Bürglin, 1997) (Supplementary Fig. S1A). A phylogenetic tree based on a trimmed alignment of StKNOX3 with eight homeobox proteins from Arabidopsis shows that StKNOX3 groups with the class II KNOX TFs (Supplementary Fig. S1B).

To confirm the interaction between Pi22798 and StKNOX3, a pairwise Y2H assay was performed with a full-length StKNOX3 prey clone against a Pi22798 bait clone, using either an empty bait, or *P. infestans* effectors PiSFI3 (Pi06087) and Pi04314, which have similar nuclear localizations *in planta* (Boevink *et al.*, 2016; He *et al.*, 2019), as controls. The nuclear-localized potato RNA-binding protein StKH17 was also included as a non-interacting control (McLellan *et al.*, 2020). Only the yeast containing both Pi22798 and StKNOX3 grew on the selection plates (-HIS) and activated the β-galactosidase (X-gal) reporter gene (Fig. 1A). To confirm that Pi22798 can interact with StKNOX3 *in planta*, Co-IP was performed by transiently co-expressing StKNOX3–GFP with HA-Pi22798 in *N. benthamiana* using agroinfiltration. HA-PiSFI3 and HA-Pi04314 were used as effector controls. All proteins were detected in the input fractions, but only the HA-Pi22798 was co-immunoprecipitated in the presence of StKNOX3–GFP (Fig. 1B) following immunoprecipitation with GFP–TRAP-M beads. A reciprocal Co-IP assay demonstrated that the Myc-StKNOX3–mRFP can be co-immunoprecipitated by GFP–Pi22798 (Supplementary Fig. S2). These results demonstrate that Pi22798 specifically interacts with StKNOX3 in yeast and *in planta*.

Pi22798 and StKNOX3 interaction occurs in the nucleoplasm

To determine where the interaction between Pi22798 and StKNOX3 occurs, vectors with RFP tags were transiently expressed in *N. benthamiana* with the nuclear marker gene GFP–StH2B (MH669357.1). Confocal images showed that StKNOX3–RFP localized in the nucleoplasm only (Fig. 2A; Supplementary Fig. S3A), whereas RFP–Pi22798 localized in the nucleoplasm and the nucleolus (Fig. 2B). Pi22798 and StKNOX3 showed different subnuclear localizations when expressed independently. When StKNOX3–GFP was co-expressed with RFP–Pi22798 in *N. benthamiana*, they co-localized in the nucleoplasm, with RFP–Pi22798 showing reduced nucleolar fluorescence, consistent with StKNOX3–GFP co-localization (Fig. 2C; Supplementary Fig. S3C). In contrast, when another tagged *P. infestans* effector, RFP–Pi04314, which strongly accumulates in the nucleoplasm and nucleolus (Boevink *et al.*, 2016), was co-expressed with StKNOX3–GFP, the nucleolar fluorescence signal of RFP–Pi04314 was unchanged (Fig. 2D). Western blots

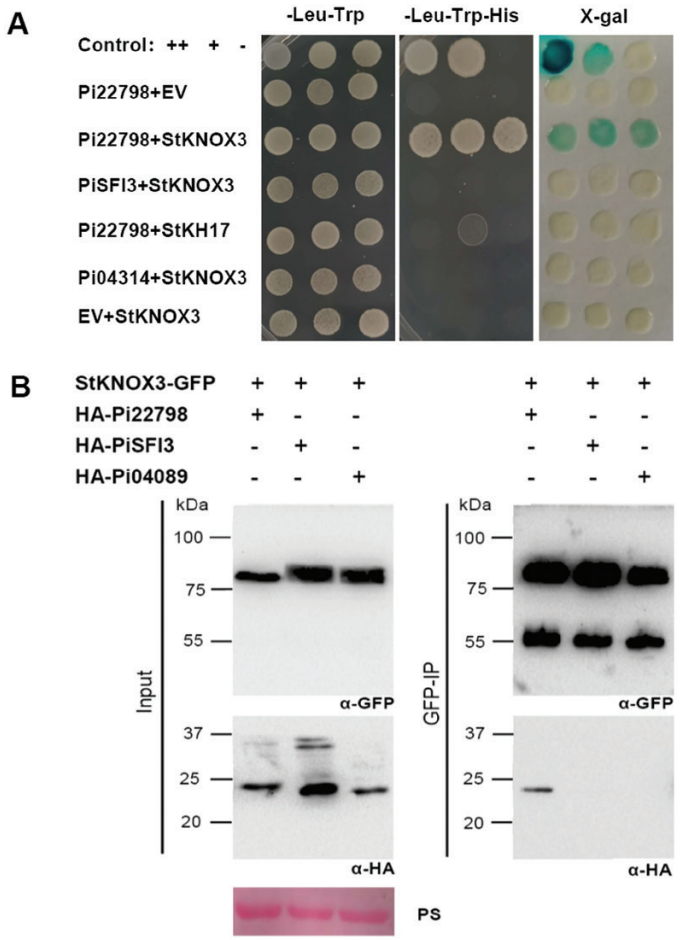

Fig. 1. Pi22798 interacts with StKNOX3 both in yeast and *in planta*. (A) Pi22798 interacts with StKNOX3 in yeast. Yeast co-expressing pDest22-StKNOX3 with pDest32-Pi22798 grew on selection medium SD/-Trp/-Leu/-His and yielded β-galactosidase (X-Gal) activity, but did not when co-expressed with the control. (B) Pi22798 interacts with StKNOX3 *in vivo*. Co-IP was performed on protein extracts from agroinfiltrated *N. benthamiana* leaves using GFP-Trap. Co-IP assays confirmed that the StKNOX3–GFP specifically associated with the HA-Pi22798, not with the controls HA-PiSFI3 or HA-Pi04314. The expression of constructions in leaves is indicated by a '+'. Protein size markers are indicated in kDa, and protein loading is indicated by Ponceau stain (PS).

were performed to show the stability of the fusion proteins (Supplementary Fig. S3B, D).

To confirm that Pi22798 and StKNOX3 interact in the nucleoplasm, a BiFC assay was conducted. The YFP N-terminal fragment (YN) was fused to Pi22798 and the YFP C-terminal fragment (YC) was fused to StKNOX3. Co-expressing YN–Pi22798 and YC–StKNOX3 resulted in YFP fluorescence restricted to the nucleoplasm, while little fluorescence was detected when co-expressing YC–StKNOX3 with YN empty vector (EV) or with YN–Pi04314 (Fig. 2E). The numbers of yellow fluorescent nuclei were quantified in replicate leaf areas in which YN–Pi22798 and YC–StKNOX3 were co-expressed, and compared with co-expression of YN-EV with YC–StKNOX3 (Fig. 2E). The results verify that Pi22798 and StKNOX3 interaction occurs in the nucleoplasm.

StKNOX3 contributes to plant susceptibility

To investigate the possible role of StKNOX3 in the host–*P. infestans* interaction, we first tested its expression pattern during *P. infestans* infection using *StKNOX3* gene-specific primers. The RT–qPCR results revealed that *StKNOX3* transcript abundance was not altered during *P. infestans* infection (Supplementary Fig. S4A, B).

To further confirm the function of StKNOX3 against the pathogen, *P. infestans* strain 88069 was inoculated onto half-leaves expressing either StKNOX3–GFP or GFP as a control. Disease lesion diameters were measured 6–7 dpi. The results showed that transient expression of StKNOX3–GFP enhances the colonization of *P. infestans* to a significant level compared with the GFP control (Fig. 3A). VIGS was employed to knock down the expression of *NbKNOX3* (the ortholog of *StKNOX3* in *N. benthamiana*, see Supplementary Fig. S1A). The 3′-UTR was selected and cloned into the TRV2 vector to produce TRV2–3′NbKNOX3 (Supplementary Fig. S5A). The silencing efficiency was measured by qRT–PCR and the transcript abundance of the target gene in TRV2–3′NbKNOX3 was reduced by 60–80% (Supplementary Fig. S5B). There were no obvious changes in phenotype between the silenced plants and control plants (Supplementary Fig. S5C). After 3 weeks, the TRV2–3′NbKNOX3 plants and TRV2–GFP control plants were inoculated with *P. infestans* strain 88069, and lesion diameters were measured. The results showed that silencing *NbKNOX3* reduced the colonization of the pathogen considerably compared with control plants (Fig. 3B).

To further confirm the negative effect of StKNOX3 upon disease resistance, stable transgenic *N. benthamiana* and potato lines were generated expressing the constructs GFP–StKNOX3 and Myc-StKNOX3–mRFP, respectively (Supplementary Figs S6, S7). Both transgenic plants displayed different growth and morphology compared with wild-type plants (Supplementary Figs S6D, S7D, E). They grew more slowly and the mature plants displayed thicker and darker green leaves. Four-week-old *N. benthamiana* leaves or 6-week-old potato leaves were used for *P. infestans* inoculation and the lesion diameters were measured. The transgenic *N. benthamiana* and potato lines sustained significantly larger disease lesions compared with the wild type (Fig. 3C, D). These results reveal that expressing StKNOX3 within host cells is beneficial to *P. infestans* colonization. All the above results indicate that StKNOX3 acts as a susceptibility (S) factor, in that it promotes and is required for efficient late blight disease development.

StKNOX3 forms a homodimer which is essential for it to promote susceptibility

It has been reported that KNOX TFs can interact with other KNOX family members to form heterodimers, or they can directly

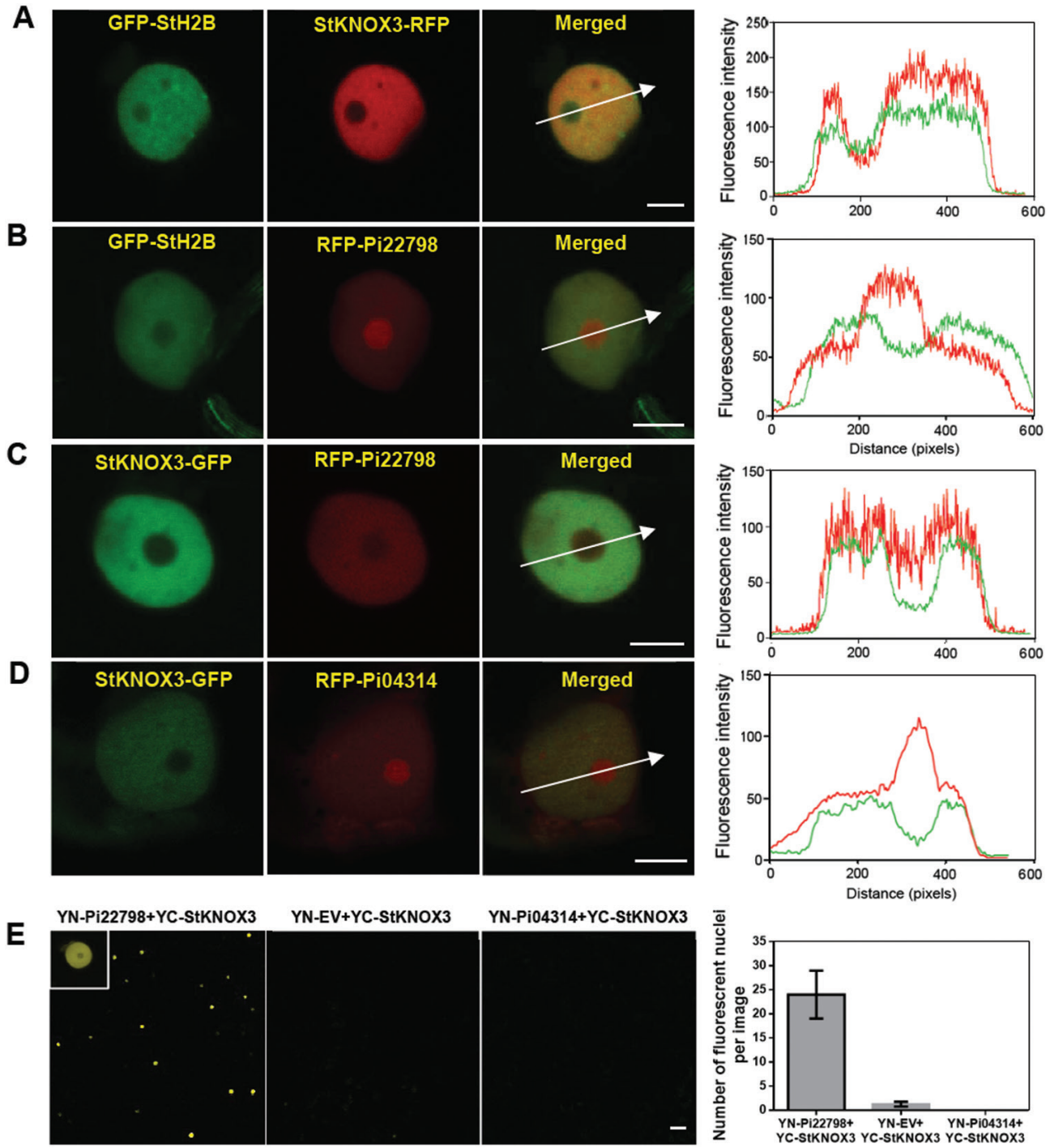

Fig. 2. Pi22798 interacts with StKNOX3 in the nucleoplasm. (A) RFP-fused StKNOX3 is expressed together with GFP–StH2B (histone 2B protein) and the RFP fluorescence mainly appears in the nucleoplasm. (B) The confocal images show that RFP–Pi22798 accumulates strongly in the nucleoplasm and the nucleolus when co-expressed with GFP–StH2B. (C) Co-expressing StKNOX3–GFP and RFP–Pi22798 shows a reduction in nucleolar fluorescence intensity for Pi22798. (D) Co-expressing StKNOX3–GFP and RFP–Pi04314 did not alter Pi04314 nucleolar intensity. Scale bar is 5 μm. Plots of the profiles indicated by the arrows in (A–D) show GFP fluorescence (green line) and mRFP signal (red line). (E) BiFC assay shows the YFP fluorescence between YN–Pi22798 and YC–StKNOX3 occurs in the nucleus. The inset image is a nucleus at higher magnification, indicating that the interaction is in the nucleoplasm specifically. Scale bar is 100 μm. The graph on the right shows the number of yellow fluorescent nuclei observed in the optical field for YN–Pi22798 and YC–StKNOX3 co-expression events, compared with co-expression with YN-EV. Error bars represent mean fluorescent nuclei number ±SD from 3–4 different optical fields.

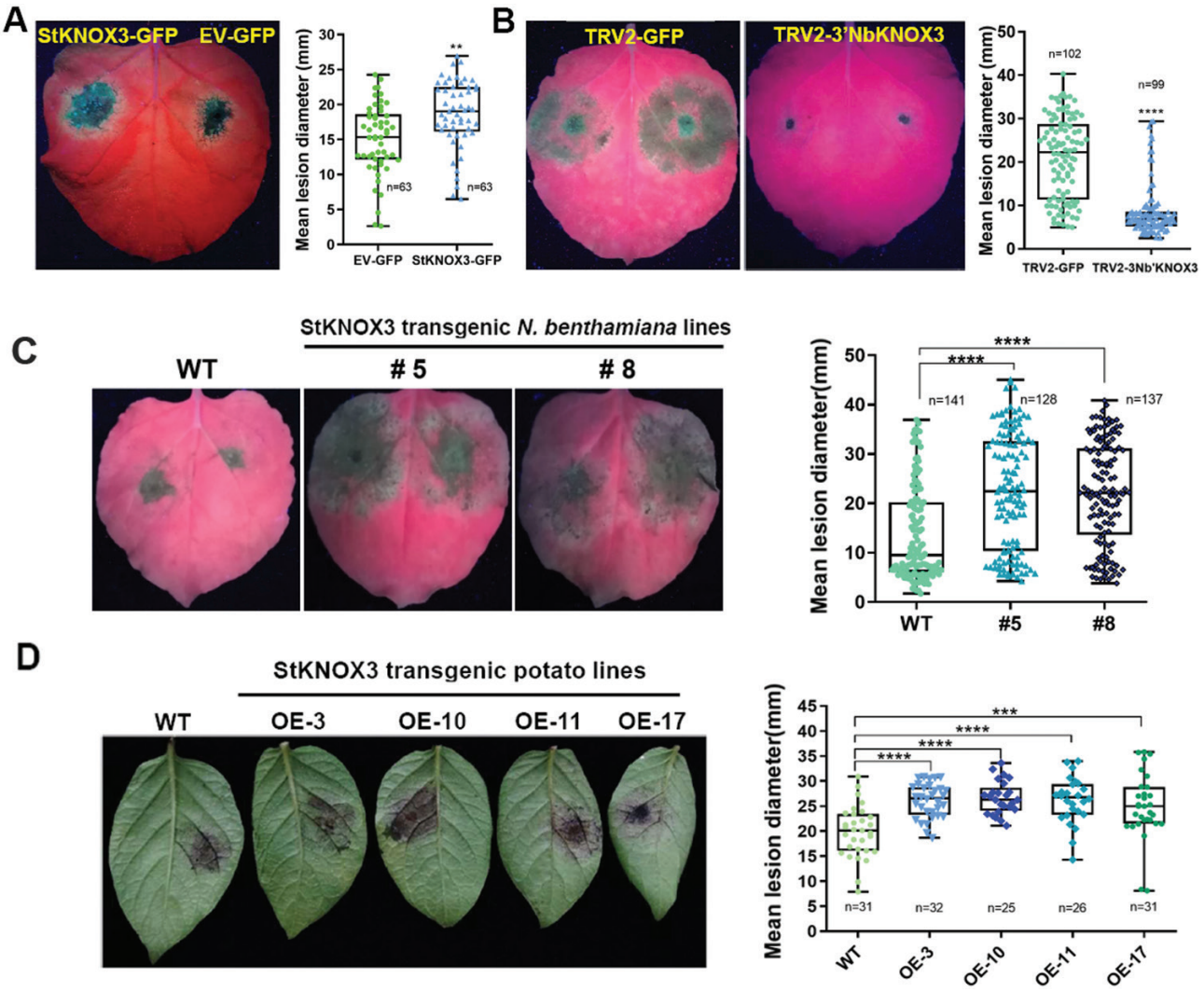

Fig. 3. StKNOX3 is an 'S' factor. (A) Graph quantifying lesion diameter in the presence or absence of StKNOX3–GFP transient expression. The image is a typical leaf showing that StKNOX3 enhances the colonization by *P. infestans* (Student's *t*-test; ****P<0.0001; three biological repeats). The data are represented as a box–whisker plot. The middle line of the boxplot represents the value of the median in the analyzed data. The upper and lower line of the boxplot represents the quartiles of each half, respectively. The lower extreme and upper extremes are the highest and lowest values in the analyzed data. The distribution of data is shown as small points or triangles. (B) Silencing *NbKNOX3* in *N. benthamiana* reduced colonization by the pathogen. Representative leaf images revealing colonization are shown above the graph. Graph showing that the lesion diameter in TRV2–3′KNOX3 plants is significantly reduced compared with TRV2–GFP control (Student's *t*-test; ****P<0.0001; three biological repeats). The data are represented as a box–whisker plot. (C) Graph shows a significant increase of lesion diameter in transgenic lines overexpressing GFP–StKNOX3 compared with wild-type plants. The representative leaves indicate more pathogen colonization on transgenic plants compared with the control plants (one-way ANOVA; ****P<0.0001; three biological repeats). The data are represented as a box–whisker plot. WT, wild type; #5 and #8, StKNOX3 transgenic *N. benthamiana* lines. (D) Graph shows a significant increase of lesion diameter in transgenic potato lines overexpressing Myc-StKNOX3–mRFP compared with wild-type plants. The representative leaves indicate more pathogen colonization on transgenic plants compared with the control plants (one-way ANOVA; ****P<0.0001; three biological repeats). The data are represented as a box–whisker plot.

associate via the KNOX II domain to form homodimers (Li *et al.*, 2011; Shu *et al.*, 2015). In Arabidopsis, KNAT3 was found to form homodimers and it could also heterodimerize with another class II KNOX protein KNAT7 (Qin *et al.*, 2020; Wang *et al.*, 2020). In rice, deletion of the KNOX II domain of OSH15 prevented it forming homodimers (Nagasaki *et al.*, 2001). StKNOX3 contains a conserved KNOX II domain as predicted (Supplementary Fig. S1A). To investigate the possible function of StKNOX3 homo-/heterodimers, a KNOX II domain deletion mutant StKNOX3$^{\Delta KNOX\ II}$ and a construct expressing the domain only, KNOX II$_{only}$, were made, and pairwise Y2H assays indicated that full-length StKNOX3 interacts with itself and StKNOX7 via binding to the KNOX II domain (KNOX II$_{only}$) directly, whereas neither interacted with the deletion mutant StKNOX3$^{\Delta KNOX\ II}$ (Fig. 4A; Supplementary

Fig. S8A). To confirm this result *in planta*, Co-IP was used following co-expression of StKNOX3–GFP, StKNOX3$^{\Delta KNOX\ II}$–GFP, or KNOX II$_{only}$–GFP with Myc-StKNOX3–mRFP or Myc-StKNOX7–mRFP in *N. benthamiana*. GFP–StKH17 was used as a control. All proteins were detected in the input fractions. Using GFP agarose beads, Myc-StKNOX3–mRFP and Myc-StKNOX7–mRFP could only be co-immunoprecipitated in the presence of StKNOX3–GFP and KNOX II$_{only}$–GFP (Fig. 4B; Supplementary Fig. S8B). StKNOX3$^{\Delta KNOX\ II}$–GFP or GFP–StKH17 do not associate with Myc-StKNOX3–mRFP or Myc-StKNOX7–mRFP (Fig. 4B; Supplementary Fig. S8B). These results demonstrate that StKNOX3 can form both homodimers and heterodimers, for which the KNOX II domain is essential and sufficient, as predicted.

As StKNOX3 enhances *P. infestans* infection, we tested whether the KNOX II domain deletion mutant altered its contribution to plant susceptibility. Myc-StKNOX3$^{\Delta KNOX\ II}$, Myc-StKNOX3, and control Myc-EV constructs were transiently expressed in *N. benthamiana* leaves. After 1 d, the infiltrated sites were inoculated with zoospores of *P. infestans* strain 88069. Lesion diameters were measured, and the results showed that the Myc-StKNOX3$^{\Delta KNOX\ II}$ deletion mutant lacked the ability to enhance colonization of *N. benthamiana* by *P. infestans*, as it showed no significant difference in lesion diameter compared with that of the Myc-EV control (Fig. 4C, D). Western blot assay confirmed their protein stabilities (Supplementary Fig. S9). This indicates that dimerization of StKNOX3 is crucial for it to act as an S factor.

The KNOX II domain is essential for StKNOX3 interaction with Pi22798 and the effector promotes homodimerization of StKNOX3

To investigate whether the KNOX II domain is required for the Pi22798–StKNOX3 interaction, a pairwise Y2H assay was performed. The results show that neither the StKNOX3$^{\Delta KNOX\ II}$ mutant

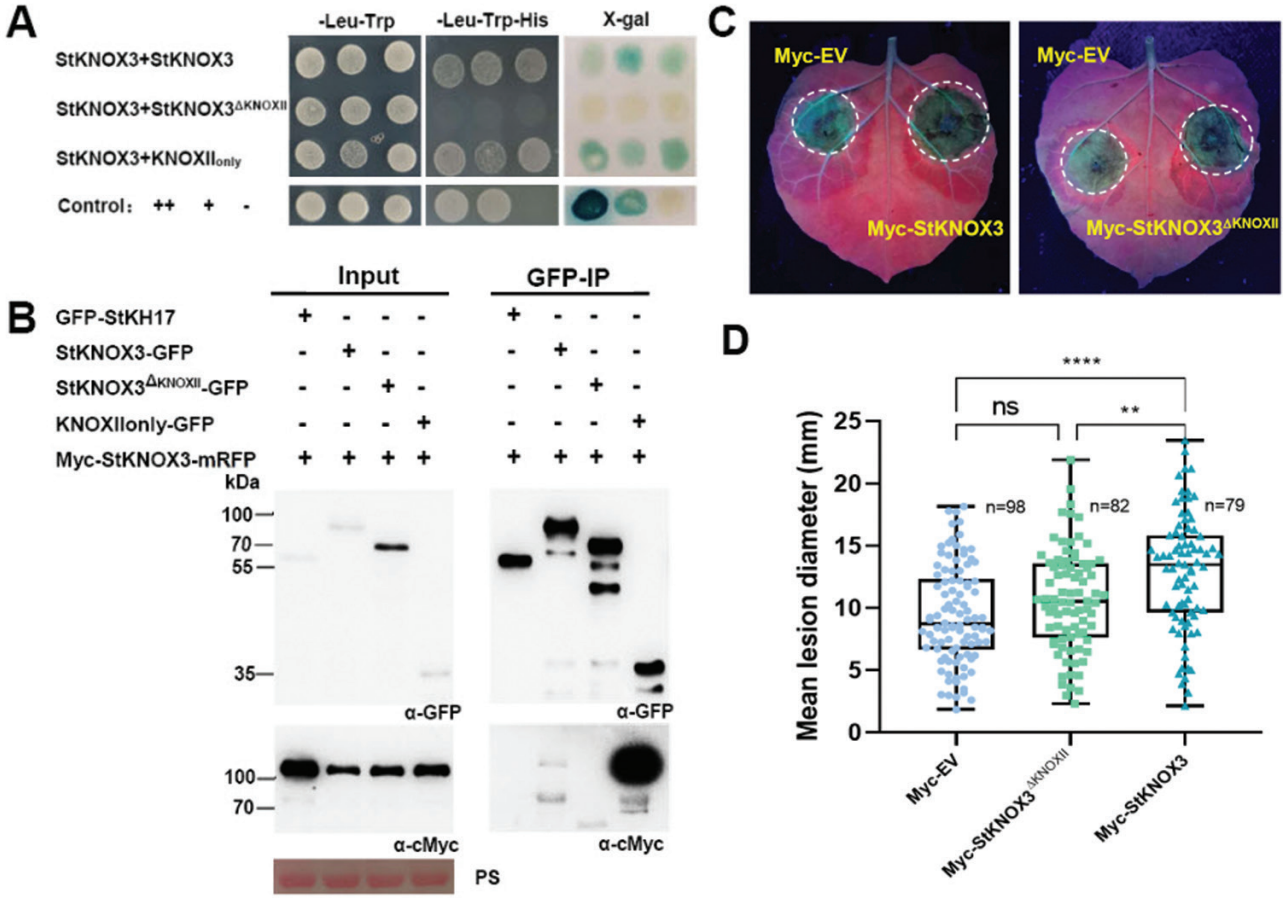

Fig. 4. StKNOX3 forms a homodimer through the KNOX II domain, which is essential for its function. (A) StKNOX3 interacts with itself in yeast and requires the KNOX II domain. Yeast co-expressing StKNOX3 with itself or KNOX II$_{only}$ grow on SD–Leu-Trp-His medium and activated the β-galactosidase (β-gal), whereas those co-expressing StKNOX3 with its deletion mutant StKNOX3$^{\Delta KNOX\ II}$ did not. (B) Co-IP from leaf extracts using GFP agarose beads confirmed that full-length Myc-StKNOX3–mRFP could be immunoprecipitated by StKNOX3–GFP and KNOX II$_{only}$–GFP, but not by deletion mutant GFP–StKNOX3$^{\Delta KNOX\ II}$ or the control GFP–StKH17. The expression of constructs in leaves is indicated by a '+'. Protein size markers are indicated in kDa, and protein loading is indicated by Ponceau stain (PS). (C) Representative leaf images showing the infection on *N. benthamiana*. (D) Graph showing that the Myc-StKNOX3$^{\Delta KNOX\ II}$ mutant lost the ability to enhance the proliferation of pathogen compared with StKNOX3 (one-way ANOVA; ns, no significant difference; ****P<0.0001; three biological repeats). The data are represented as a box–whisker plot.

nor the KNOX II_{only} domain alone interacted with Pi22798 in yeast (Fig. 5A). To confirm these results *in planta*, two Co-IP assays were performed. As shown in Fig. 5B and C, Pi22798 was only co-immunoprecipitated with StKNOX3, but not with the $StKNOX3^{\Delta KNOX\ II}$ or KNOX II_{only} mutant, or the control StKH17. These results demonstrate that the KNOX II domain is essential but not sufficient for StKNOX3 to interact with Pi22798.

We have shown that the ability of StKNOX3 to form dimers is required for it to enhance susceptibility to *P. infestans* (Fig. 4C, D). In addition, the KNOX II domain is required for the interaction with Pi22798 (Fig. 5). We thus tested whether Pi22798 affects the dimerization of StKNOX3. A Co-IP assay was conducted in which StKNOX3–GFP was co-expressed with Myc-StKNOX3–mRFP in the presence or absence of HA-Pi22798. Myc-StKNOX3–mRFP was co-immunoprecipitated by StKNOX3–GFP, not by the control GFP–β-glucuronidase (GUS) (Fig. 6A). In addition, HA-Pi22798 was also co-immunoprecipitated by StKNOX3–GFP. Critically, more Myc-StKNOX3–mRFP protein was pulled down by StKNOX3–GFP in the presence than in the absence of HA-Pi22798, whereas all proteins were present in the relevant input fractions in similar amounts (Fig. 6A). An additional two experimental Co-IP repeats are in accordance with this result (Supplementary Fig. S10). Moreover, we observed that another *P. infestans* effector PiSFI3 does not promote StKNOX3 dimerization (Supplementary Fig. S10B). In addition, the split-LUC assay was also used to confirm the conclusion. Repeated results showed that Pi22798, but not PiSFI3, significantly enhances the interaction of StKNOX3 with itself, reflected by stronger fluorescence intensity when StKNOX3–nLUC and cLUC–StKNOX3 were co-expressed with Pi22798. StKNOX3–nLUC with cLUC–StKH17 or nLUC with cLUC–StKNOX3 were used as negative control (Fig. 6B, C; Supplementary Fig. S11). The protein stability of the split-LUC constructs was detected using western blot (Supplementary Fig. S12). These results demonstrate that the effector Pi22798 promotes homodimerization of StKNOX3.

As StKNOX3 also forms a heterodimer with StKNOX7, which also requires the KNOX II domain, we investigated whether Pi22798 alters their heterodimerization. To test this hypothesis, Co-IPs from leaf extracts co-expressing StKNOX7–GFP and Myc-StKNOX3–mRFP in the presence of different concentrations of HA-Pi22798 were conducted. However, even with increased concentration of HA-Pi22798, the amount of Myc-StKNOX3–mRFP immunoprecipited by StKNOX7–GFP showed no obvious difference (Supplementary Fig. S13), suggesting that the effector Pi22798 did not affect the heterodimerization of StKNOX3 and StKNOX7. This provides independent evidence supporting the hypothesis that Pi22798 promotes homodimerization of StKNOX3 rather than heterodimerization of StKNOX3 and StKNOX7 *in planta*.

Discussion

The nucleus is a pivotal site for the plant to activate innate immunity to prevent diverse pathogen attacks. Accordingly, oomycete pathogens have evolved effectors which are delivered to the plant nucleus to manipulate immunity and enhance infection. In a previous study, the nuclear effector Pi22798 was revealed to be up-regulated during early stages of infection of potato by *P. infestans*, and transient expression of Pi22798 contributes to the infection of *P. infestans* in *N. benthamiana* leaves (H. Wang *et al.*, 2017). It has been shown that the nuclear localization is essential for Pi22798 to fulfill its virulence function, implying that its targets may be located in the host nucleus (H. Wang *et al.*, 2017). Here, we identified a homeobox TF, StKNOX3, as a likely target (Fig. 1). Co-localization of fluorescently tagged Pi22798 and StKNOX3, and BiFC, indicate that the interaction occurs in the nucleoplasm (Fig. 2) as anticipated. We show that transient and stable expression of StKNOX3 in *N. benthamiana* enhanced *P. infestans* leaf colonization, whereas silencing *NbKNOX3* in *N. benthamiana* leaves dramatically reduced *P. infestans* colonization, consistent with it playing a role as a susceptibility (S) factor, in that it is required for full disease development (Fig. 3).

Pi22798 accumulates in the nucleoplasm when co-expressed with StKNOX3 (Fig. 2). Some pathogen effectors re-localize their targets, which is important for their virulence activity. For example, *Phytophthora sojae* PsAvh52 re-localizes GmTAP1 into the nucleus, leading to histone acetylation during early infection (Li *et al.*, 2018). The *P. infestans* effector Pi04314 interacts with three PP1c isoforms, causing their re-localization from the nucleolus to the nucleoplasm (Boevink *et al.*, 2016). Moreover, *P. infestans* effector Pi03192 prevents elicitor-triggered re-localization of two potato NAC transcript factors, StNTP1 and StNTP2, from the endoplasmic reticulum (ER) into the nucleus, thus preventing their transcriptional activity (McLellan *et al.*, 2013). The *P. sojae* effector PsAvh262 interacts with and stabilizes BiPs at the ER, leading to suppression of ER stress-mediated immunity (Jing *et al.*, 2016). Here we display a situation in which the effector Pi22798 accumulates at the site of its interacting host target, StKNOX3, perhaps indicating that this effector promotes transcriptional regulation caused by StKNOX3, especially as the latter positively contributes to susceptibility (Fig. 3).

It has been reported that pathogen effectors can modulate nuclear functions by interacting with host TFs. For example, a CRN effector from *Phytophthora capsici* binds to a TCP TF, SlTCP14-2, to diminish its chromatin affinity, thus enhancing susceptibility (Stam *et al.*, 2021). A *Xanthomonas* type III secretion effector XopD desumoylates the tomato ethylene-responsive TF SlERF4 to repress ethylene production which is required for anti-Xcv immunity (J.G. Kim *et al.*, 2013). GSRE1 from *Puccinia striiformis* f. sp. *tritici* interacts with a reactive oxygen species-related TF, TaLOL2, whose nuclear localization was disrupted when co-expressed with the effector, thus suppressing the cell death induced by TaLOL2 and promoting susceptibility (Qi *et al.*, 2019). Oomycete effector HaRxLL470 enhances pathogenicity by interacting with a bZIP TF AtHY5 to suppress its transcriptional activation of defense-related genes (Chen *et al.*, 2021). In this study, the target of Pi22798 belongs to the KNOX TF family. This

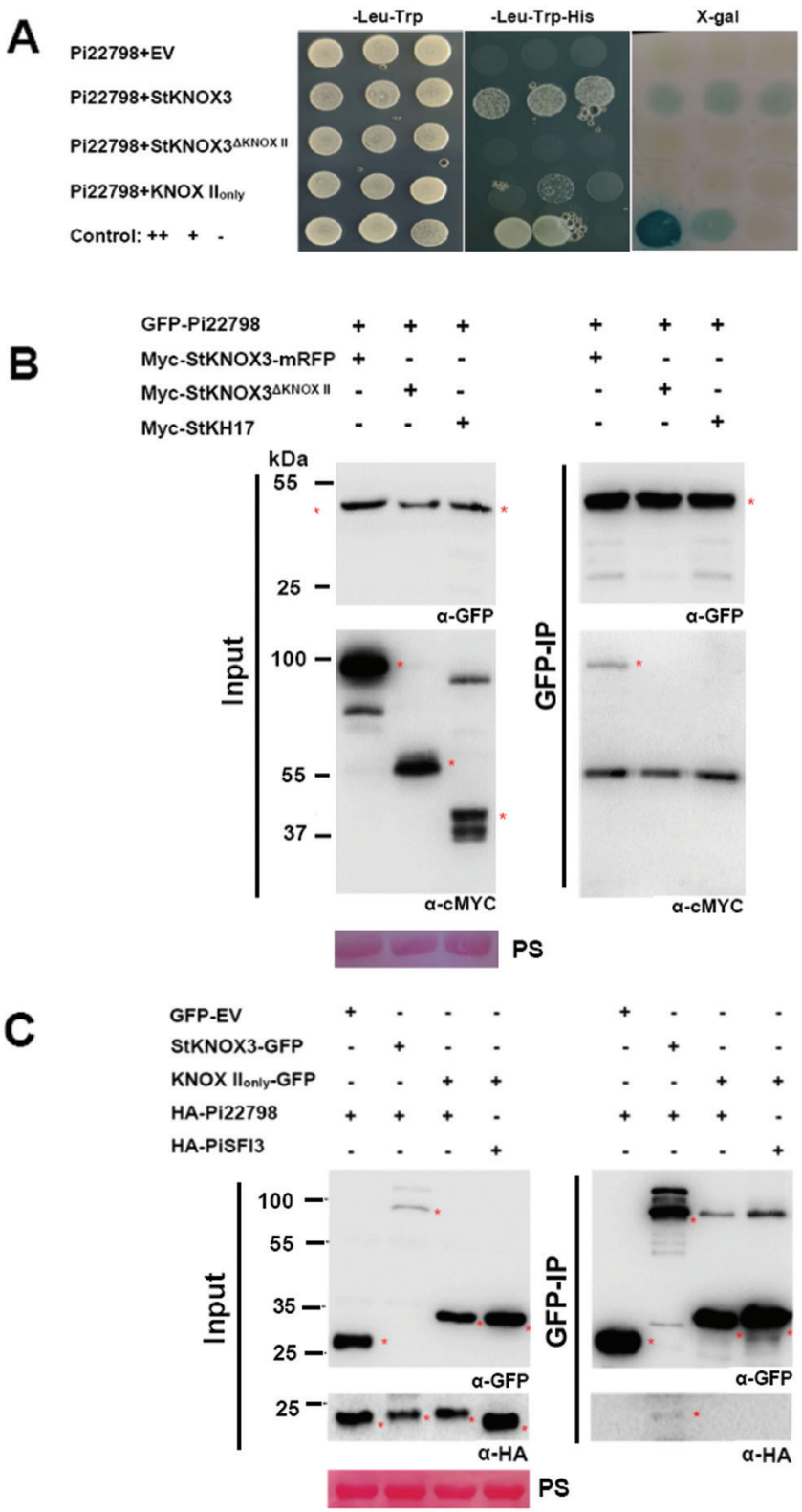

Fig. 5. Pi22798 interacts with StKNOX3 through binding the KNOX II domain indirectly. (A) Yeast containing Pi22798 and full-length StKNOX3 grew on SD-Leu-Trp-His medium and had β-galactosidase (X-gal) activity, whereas those co-expressing Pi22798 with the deletion mutant StKNOX3$^{\Delta KNOX\ II}$, KNOX II$_{only}$, or empty vector did not. (B) Co-IP from leaf extracts using the GFP trap confirmed that GFP–Pi22798 co-immunoprecipitated only with wild-type Myc-StKNOX3–RFP. (C) Co-IP from leaf extracts using the GFP trap confirmed that HA-Pi22798 co-immunoprecipitated only with StKNOX3–GFP, not with KNOX II$_{only}$–GFP. The expression of constructs in leaves is indicated by a '+'. Protein size markers are indicated in kDa, and protein loading is indicated by Ponceau stain (PS). The target bands were marked by '*'.

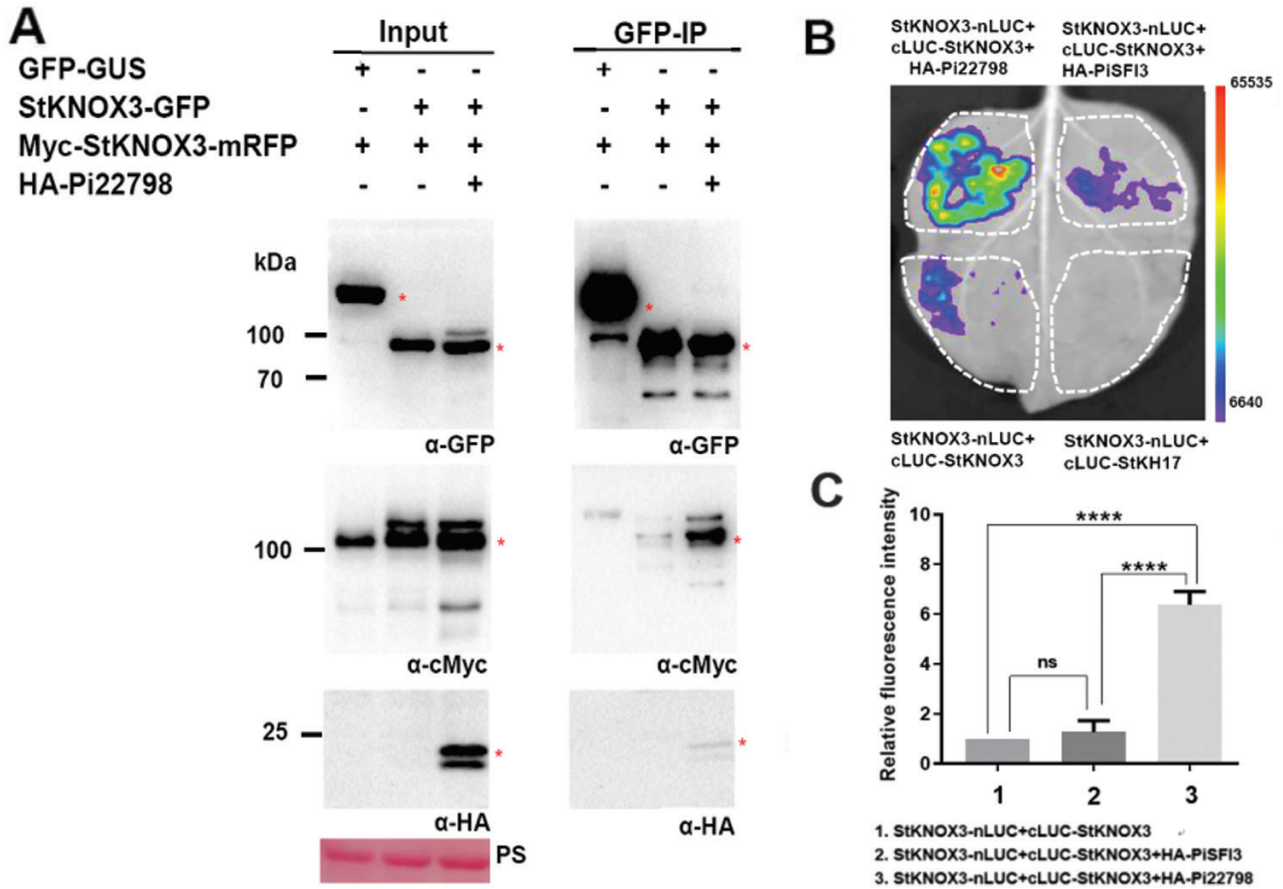

Fig. 6. Pi22798 promotes dimerization of StKNOX3. (A) Co-IP experiment showing that GFP–StKNOX3 immunoprecipitated more Myc-StKNOX3–mRFP proteins in the presence of HA-Pi22798. The expression of constructs in leaves is indicated by a '+'. Protein size markers are indicated in kDa, and protein loading is indicated by Ponceau stain (PS). The target bands were marked by '*'. (B) Split luciferase complementation experiments confirmed that Pi22798 promoted the homodimerization of StKNOX3 *in planta*. The four circled quadrants show different combinations of expressed constructs. (C) Quantitative statistics of fluorescence intensity of interaction between cLUC–StKNOX3 and StKNOX3–nLUC. The fluorescence intensity of StKNOX3–nLUC and cLUC–StKNOX3 was normalized to 1 and error bars indicate the mean ±SEM (n=7). Asterisks indicate the difference in fluorescence intensity in the presence of HA-Pi22798 or HA-PiSFI3 (****P<0.0001). Statistical analysis was carried out using ANOVA with pairwise comparisons performed with a Holm–Sidak test.

family of proteins contain four conserved domains which perform different functions. The KNOX I domain plays a role in suppressing transcriptional auto-activation, whereas the KNOX II domain is required for homo-/heterodimerization (Nagasaki *et al.*, 2001; Shu *et al.*, 2015). Using Y2H, Co-IP, and split-LUC, we found that the KNOX II domain is essential for StKNOX3 to form homo-/heterodimers and that this is also essential for it to promote susceptibility and interact with Pi22798. Moreover, our results show that Pi22798 promotes homodimerization of StKNOX3, but not its heterodimerization to StKNOX7, implying that the effector uses this strategy to manipulate host transcription. Interestingly, a recent observation showed that an RXLR effector, PsAvh241, inhibits plant ETI by preventing the dimerization of the positive immune regulator, GmNDR1 (Yang *et al.*, 2021). Promoting or preventing dimerization of host proteins is thus a strategy for manipulating host susceptibility.

To date, most KNOX protein studies have focused on their roles in plant growth and development, including leaf morphology, germination, and early seedling development (Vollbrecht *et al.*, 1991; Shani *et al.*, 2009; Yu *et al.*, 2021). However, the functions of class II KNOX TFs and their regulated genes have not been well established. The Gene Ontology (GO) analysis of the *knat3* mutant in Arabidopsis showed that the up-regulated differentially expressed genes (DEGs) are mainly involved in lipid catabolic processes, xyloglucan metabolic processes, wax biosynthetic processes, and cell wall organization, while the down-regulated DEGs participate in responses to phytohormone, and abiotic and biotic stimulants (Qin *et al.*, 2020). KNAT3 was shown to heterodimerize with KNAT7 to regulate monolignol biosynthesis and secondary cell wall biosynthesis in Arabidopsis (Qin *et al.*, 2020; Wang *et al.*, 2020), which could impact plant immunity. Our data also indicated the StKNOX3 forms a heterodimer with StKNOX7

in planta (Supplementary Fig. S8). However, critically, the effector Pi22798 promotes StNOX3 homodimerization, rather than heterodimerization to StKNOX7. It is plausible that StKNOX3 also plays a role in the development of the plant cell wall in potato. To further investigate the function of Pi22798 in manipulating plant defense, future studies are required to determine the targeted genes of StKNOX3 homodimers, and how these genes enhance susceptibility.

Supplementary data

The following Supplementary data are available at *JXB* online.

Table S1. Primers used in this study.

Fig. S1. Alignment of KNOX3 paralogs and phylogenetic tree of Arabidopsis and *S. tuberosum* KNOX3 transcription factor sequences.

Fig. S2. StKNOX3 interacts with Pi22798 *in planta*.

Fig. S3. Additional images showing that StKNOX3 and Pi22798 cause relocalization of Pi22798 specifically to the nucleoplasm (as in Fig. 2A).

Fig. S4. StKNOX3 is not responsive to *P. infestans* infection.

Fig. S5. Silencing efficiency of the TRV2-*NbKNOX3* construct.

Fig. S6. Phenotypes of stable *GFP-StKNOX3* transgenic *N. benthamiana* plants.

Fig. S7. Phenotypes of stable *StKNOX3* transgenic potato plants.

Fig. S8. StKNOX3 forms a heterodimer with StKNOX7 and their association relies on the KNOX II domain.

Fig. S9. Protein stability of Myc-StKNOX3 and Myc-StKNOX3$^{\Delta KNOXII}$ constructs.

Fig. S10. Two additional repeats showing that effector Pi22798 promotes dimerization of StKNOX3 using Co-IP (as in Fig. 6A).

Fig. S11. Six additional repeats showing that effector Pi22798 promotes dimerization of StKNOX3 using spilt-LUC (as in Fig. 6B).

Fig. S12. Protein stability of spilt-LUC constructs.

Fig. S13. Effector Pi22798 does not promote the heterodimerization of StKNOX3 and StKNOX7.

Author contributions

TZ, PRJB, PCB, and ZJ: planning and design; ZJ, QY, NJ, GL, and LM: performing experiments and data analysis; ZJ, HM, PRJB, and ZT: writing with input from all authors.

Conflict of interest

The authors have no conflicts to declare.

Funding

The National Natural Science Foundation of China (grant nos 32072121 and 31761143007); Biotechnology and Biological Sciences Research Council grants BB/P020569/1, BB/N009967/1, and BB/L026880/1; ERC-Advanced grant PathEVome (787764); and Scottish Government Rural and Environment Science and Analytical Services Division (RESAS).

Data availability

The data that support the findings of this study are available in the supplementary data of this article.

References

Azarakhsh M, Kirienko AN, Zhukov VA, Lebedeva MA, Dolgikh EA, Lutova LA. 2015. KNOTTED1-LIKE HOMEOBOX 3: a new regulator of symbiotic nodule development. Journal of Experimental Botany **66**, 7181–7195.

Azarakhsh M, Rumyantsev AM, Lebedeva MA, Lutova LA. 2020. Cytokinin biosynthesis genes expressed during nodule organogenesis are directly regulated by the KNOX3 protein in *Medicago truncatula*. PLoS One **15**, e0232352.

Belles-Boix E, Hamant O, Witiak SM, Morin H, Traas J, Pautot V. 2006. *KNAT6*: an Arabidopsis homeobox gene involved in meristem activity and organ separation. The Plant Cell **18**, 1900–1907.

Bertolino E, Reimund B, Wildt-Perinic D, Clerc RG. 1995. A novel homeobox protein which recognizes a TGT core and functionally interferes with a retinoid-responsive motif. Journal of Biological Chemistry **270**, 31178–31188.

Bhargava A, Ahad A, Wang S, Mansfield SD, Haughn GW, Douglas CJ, Ellis BE. 2013. The interacting MYB75 and KNAT7 transcription factors modulate secondary cell wall deposition both in stems and seed coat in Arabidopsis. Planta **237**, 1199–1211.

Boevink PC, Wang X, McLellan H, *et al*. 2016. A *Phytophthora infestans* RXLR effector targets plant PP1c isoforms that promote late blight disease. Nature Communications **7**, 10311.

Bos JI, Armstrong MR, Gilroy EM, *et al*. 2010. *Phytophthora infestans* effector AVR3a is essential for virulence and manipulates plant immunity by stabilizing host E3 ligase CMPG1. Proceedings of the National Academy of Sciences, USA **107**, 9909–9914.

Brown DM, Zeef LA, Ellis J, Goodacre R, Turner SR. 2005. Identification of novel genes in Arabidopsis involved in secondary cell wall formation using expression profiling and reverse genetics. The Plant Cell **17**, 2281–2295.

Brunner F, Rosahl S, Lee J, Rudd JJ, Geiler C, Kauppinen S, Rasmussen G, Scheel D, Nürnberger T. 2002. Pep-13, a plant defense-inducing pathogen-associated pattern from *Phytophthora* transglutaminases. The EMBO Journal **21**, 6681–6688.

Bürglin TR. 1997. Analysis of TALE superclass homeobox genes (MEIS, PBC, KNOX, Iroquois, TGIF) reveals a novel domain conserved between plants and animals. Nucleic Acids Research **25**, 4173–4180.

Byrne ME, Simorowski J, Martienssen RA. 2002. ASYMMETRIC LEAVES1 reveals knox gene redundancy in Arabidopsis. Development **129**, 1957–1965.

Chen S, Ma T, Song S, *et al*. 2021. Arabidopsis downy mildew effector HaRxLL470 suppresses plant immunity by attenuating the DNA-binding activity of bZIP transcription factor HY5. New Phytologist **230**, 1562–1577.

Chinchilla D, Bauer Z, Regenass M, Boller T, Felix G. 2006. The Arabidopsis receptor kinase FLS2 binds flg22 and determines the specificity of flagellin perception. The Plant Cell **18**, 465–476.

Di Giacomo E, Laffont C, Sciarra F, Iannelli MA, Frugier F, Frugis G. 2017. KNAT3/4/5-like class 2 KNOX transcription factors are involved in *Medicago truncatula* symbiotic nodule organ development. New Phytologist **213**, 822–837.

Dockx J, Quaedvlieg N, Keultjes G, Kock P, Weisbeek P, Smeekens S. 1995. The homeobox gene *ATK1* of *Arabidopsis thaliana* is expressed in the shoot apex of the seedling and in flowers and inflorescence stems of mature plants. Plant Molecular Biology **28**, 723–737.

Dodds PN, Rathjen JP. 2010. Plant immunity: towards an integrated view of plant–pathogen interactions. Nature Reviews Genetics **11**, 539–548.

Douglas SJ, Chuck G, Dengler RE, Pelecanda L, Riggs CD. 2002. KNAT1 and ERECTA regulate inflorescence architecture in Arabidopsis. The Plant Cell **14**, 547–558.

Du Y, Chen X, Guo Y, Zhang X, Zhang H, Li F, Huang G, Meng Y, Shan W. 2021. *Phytophthora infestans* RXLR effector PITG20303 targets a potato MKK1 protein to suppress plant immunity. New Phytologist **229**, 501–515.

Ehlting J, Mattheus N, Aeschliman DS, *et al*. 2005. Global transcript profiling of primary stems from *Arabidopsis thaliana* identifies candidate genes for missing links in lignin biosynthesis and transcriptional regulators of fiber differentiation. The Plant Journal **42**, 618–640.

Fry WE, Birch PR, Judelson HS, *et al*. 2015. Five reasons to consider *Phytophthora infestans* a reemerging pathogen. Phytopathology **105**, 966–981.

Fu DQ, Zhu BZ, Zhu HL, Jiang WB, Luo YB. 2005. Virus-induced gene silencing in tomato fruit. The Plant Journal **43**, 299–308.

Haas BJ, Kamoun S, Zody MC, *et al*. 2009. Genome sequence and analysis of the Irish potato famine pathogen *Phytophthora infestans*. Nature **461**, 393–398.

Hackbusch J, Richter K, Müller J, Salamini F, Uhrig JF. 2005. A central role of *Arabidopsis thaliana* ovate family proteins in networking and subcellular localization of 3-aa loop extension homeodomain proteins. Proceedings of the National Academy of Sciences, USA **102**, 4908–4912.

Hay A, Tsiantis M. 2010. KNOX genes: versatile regulators of plant development and diversity. Development **137**, 3153–3165.

He Q, McLellan H, Boevink PC, Birch PRJ. 2020. All roads lead to susceptibility: the many modes of action of fungal and oomycete intracellular effectors. Plant Communications **1**, 100050.

He Q, McLellan H, Hughes RK, Boevink PC, Armstrong M, Lu Y, Banfield MJ, Tian Z, Birch PRJ. 2019. *Phytophthora infestans* effector SFI3 targets potato UBK to suppress early immune transcriptional responses. New Phytologist **222**, 438–454.

He Q, Naqvi S, McLellan H, Boevink PC, Champouret N, Hein I, Birch PRJ. 2018. Plant pathogen effector utilizes host susceptibility factor NRL1 to degrade the immune regulator SWAP70. Proceedings of the National Academy of Sciences, USA **115**, E7834–E7843.

Huang D, Wang S, Zhang B, *et al*. 2015. A gibberellin-mediated DELLA–NAC signaling cascade regulates cellulose synthesis in rice. The Plant Cell **27**, 1681–1696.

Jing M, Guo B, Li H, *et al*. 2016. A *Phytophthora sojae* effector suppresses endoplasmic reticulum stress-mediated immunity by stabilizing plant binding immunoglobulin proteins. Nature Communications **7**, 11685.

Jones JDG, Dangl JL. 2006. The plant immune system. Nature **444**, 323–329.

Kamoun S, Furzer O, Jones JD, *et al*. 2015. The Top 10 oomycete pathogens in molecular plant pathology. Molecular Plant Pathology **16**, 413–434.

Kerstetter R, Vollbrecht E, Lowe B, Veit B, Yamaguchi J, Hake S. 1994. Sequence analysis and expression patterns divide the maize knotted1-like homeobox genes into two classes. The Plant Cell **6**, 1877–1887.

Kim D, Cho YH, Ryu H, Kim Y, Kim TH, Hwang I. 2013. BLH1 and KNAT3 modulate ABA responses during germination and early seedling development in Arabidopsis. The Plant Journal **75**, 755–766.

Kim JG, Stork W, Mudgett MB. 2013. *Xanthomonas* type III effector XopD desumoylates tomato transcription factor SlERF4 to suppress ethylene responses and promote pathogen growth. Cell Host and Microbe **13**, 143–154.

King SR, McLellan H, Boevink PC, Armstrong MR, Bukharova T, Sukarta O, Win J, Kamoun S, Birch PR, Banfield MJ. 2014. *Phytophthora infestans* RXLR effector PexRD2 interacts with host MAPKKK ε to suppress plant immune signaling. The Plant Cell **26**, 1345–1359.

Li E, Wang S, Liu Y, Chen JG, Douglas CJ. 2011. OVATE FAMILY PROTEIN4 (OFP4) interaction with KNAT7 regulates secondary cell wall formation in *Arabidopsis thaliana*. The Plant Journal **67**, 328–341.

Li H, Wang H, Jing M, *et al*. 2018. A *Phytophthora* effector recruits a host cytoplasmic transacetylase into nuclear speckles to enhance plant susceptibility. eLife **7**, e40039.

Liu Y, Douglas CJ. 2015. A role for OVATE FAMILY PROTEIN1 (OFP1) and OFP4 in a BLH6–KNAT7 multi-protein complex regulating secondary cell wall formation in *Arabidopsis thaliana*. Plant Signaling & Behavior **10**, e1033126.

Liu Y, You S, Taylor-Teeples M, Li WL, Schuetz M, Brady SM, Douglas CJ. 2014. BEL1-LIKE HOMEODOMAIN6 and KNOTTED ARABIDOPSIS THALIANA7 interact and regulate secondary cell wall formation *via* repression of REVOLUTA. The Plant Cell **12**, 4843–4861.

Livak K, Schmittgen T. 2001. Analysis of relative gene expression data using real-time quantitative PCR and the $2^{-\Delta\Delta CT}$ method. Methods **25**, 402–408.

Long JA, Moan EI, Medford JI, Barton MK. 1996. A member of the KNOTTED class of homeodomain proteins encoded by the STM gene of Arabidopsis. Nature **379**, 66–69.

McLellan H, Boevink PC, Armstrong MR, Pritchard L, Gomez S, Morales J, Whisson SC, Beynon JL, Birch PR. 2013. An RxLR effector from *Phytophthora infestans* prevents re-localisation of two plant NAC transcription factors from the endoplasmic reticulum to the nucleus. PLoS Pathogens **9**, e1003670.

McLellan H, Chen K, He Q, Wu X, Boevink PC, Tian Z, Birch PRJ. 2020. The ubiquitin E3 ligase PUB17 positively regulates immunity by targeting a negative regulator, KH17, for degradation. Plant Communications **1**, 100020.

Mukherjee K, Brocchieri L, Bürglin TR. 2009. A comprehensive classification and evolutionary analysis of plant homeobox genes. Molecular Biology and Evolution **26**, 2775–2794.

Nagasaki H, Sakamoto T, Sato Y, Matsuoka M. 2001. Functional analysis of the conserved domains of a rice KNOX homeodomain protein, OSH15. The Plant Cell **13**, 2085–2098.

Pagnussat GC, Yu HJ, Sundaresan V. 2007. Cell-fate switch of synergid to egg cell in *Arabidopsis eostre* mutant embryo sacs arises from misexpression of the BEL1-like homeodomain gene *BLH1*. The Plant Cell **19**, 3578–3592.

Persson S, Wei H, Milne J, Page GP, Somerville CR. 2005. Identification of genes required for cellulose synthesis by regression analysis of public microarray data sets. Proceedings of the National Academy of Sciences, USA **102**, 8633–8638.

Qi T, Guo J, Liu P, He F, Wan C, Islam MA, Tyler BM, Kang Z, Guo J. 2019. Stripe rust effector PstGSRE1 disrupts nuclear localization of ROS-promoting transcription factor TaLOL2 to defeat ROS-induced defense in wheat. Molecular Plant **12**, 1624–1638.

Qin W, Yin Q, Chen J, *et al*. 2020. The class II KNOX transcription factors KNAT3 and KNAT7 synergistically regulate monolignol biosynthesis in Arabidopsis. Journal of Experimental Botany **71**, 5469–5483.

Ragni L, Belles-Boix E, Günl M, Pautot V. 2008. Interaction of KNAT6 and KNAT2 with BREVIPEDICELLUS and PENNYWISE in Arabidopsis inflorescences. The Plant Cell **20**, 888–900.

Ren Y, Armstrong M, Qi Y, McLellan H, Zhong C, Du B, Birch PRJ, Tian Z. 2019. *Phytophthora infestans* RXLR effectors target parallel steps in an immune signal transduction pathway. Plant Physiology **180**, 2227–2239.

Shani E, Burko Y, Ben-Yaakov L, Berger Y, Amsellem Z, Goldshmidt A, Sharon E, Ori N. 2009. Stage-specific regulation of *Solanum lycopersicum* leaf maturation by class 1 KNOTTED1-LIKE HOMEOBOX proteins. The Plant Cell **21**, 3078–3092.

Shu Y, Tao Y, Wang S, Huang L, Yu X, Wang Z, Chen M, Gu W, Ma H. 2015. *GmSBH1*, a homeobox transcription factor gene, relates to growth and development and involves in response to high temperature and humidity stress in soybean. Plant Cell Reports **34**, 1927–1937.

Sinha NR, Williams RE, Hake S. 1993. Overexpression of the maize homeo box gene, *KNOTTED-1*, causes a switch from determinate to indeterminate cell fates. Genes & Development **7**, 787–795.

Smaczniak C, Immink RG, Muiño JM, *et al*. 2012. Characterization of MADS-domain transcription factor complexes in Arabidopsis flower

development. Proceedings of the National Academy of Sciences, USA **109**, 1560–1565.

Stam R, Motion GB, Martinez-Heredia V, Boevink PC, Huitema E. 2021. A conserved oomycete CRN effector targets tomato TCP14-2 to enhance virulence. Molecular Plant-Microbe Interactions **34**, 309–318.

Vollbrecht E, Veit B, Sinha N, Hake S. 1991. The developmental gene *Knotted-1* is a member of a maize homeobox gene family. Nature **350**, 241–243.

Wang H, Ren Y, Zhou J, Du J, Hou J, Jiang R, Wang H, Tian Z, Xie C. 2017. The cell death triggered by the nuclear localized RxLR effector PITG_22798 from *Phytophthora infestans* is suppressed by the effector AVR3b. International Journal of Molecular Sciences **18**, 409.

Wang S, Boevink PC, Welsh L, Zhang R, Whisson SC, Birch PRJ. 2017. Delivery of cytoplasmic and apoplastic effectors from *Phytophthora infestans* haustoria by distinct secretion pathways. New Phytologist **216**, 205–215.

Wang S, McLellan H, Bukharova T, *et al*. 2019a. *Phytophthora infestans* RXLR effectors act in concert at diverse subcellular locations to enhance host colonization. Journal of Experimental Botany **70**, 343–356.

Wang S, Welsh L, Thorpe P, Whisson SC, Boevink PC, Birch PRJ. 2018. The *Phytophthora infestans* haustorium is a site for secretion of diverse classes of infection-associated proteins. mBio **9**, e01216–e01218.

Wang S, Yamaguchi M, Grienenberger E, Martone PT, Samuels AL, Mansfield SD. 2020. The Class II KNOX genes KNAT3 and KNAT7 work cooperatively to influence deposition of secondary cell walls that provide mechanical support to Arabidopsis stems. The Plant Journal **101**, 293–309.

Wang S, Yang H, Mei J, Liu X, Wen Z, Zhang L, Xu Z, Zhang B, Zhou Y. 2019b. Rice homeobox protein KNAT7 integrates the pathways regulating cell expansion and wall stiffness. Plant Physiology **181**, 669–682.

Wang X, Boevink P, McLellan H, Armstrong M, Bukharova T, Qin Z, Birch PR. 2015. A host KH RNA-binding protein is a susceptibility factor targeted by an RXLR effector to promote late blight disease. Molecular Plant **8**, 1385–1395.

Whisson SC, Boevink PC, Wang S, Birch PRJ. 2016. The cell biology of late blight disease. Current Opinion in Microbiology **34**, 127–135.

Win J, Krasileva KV, Kamoun S, Shirasu K, Staskawicz BJ, Banfield MJ. 2012. Sequence divergent RXLR effectors share a structural fold conserved across plant pathogenic oomycete species. PLoS Pathogens **8**, e1002400.

Yang B, Yang S, Guo B, *et al*. 2021. The Phytophthora effector Avh241 interacts with host NDR1-like proteins to manipulate plant immunity. Journal of Integrative Plant Biology **63**, 1382–1396.

Yang L, McLellan H, Naqvi S, *et al*. 2016. Potato NPH3/RPT2-like protein StNRL1, targeted by a *Phytophthora infestans* RXLR effector, is a susceptibility factor. Plant Physiology **171**, 645–657.

Yu H, Zhang L, Wang W, *et al*. 2021. TCP5 controls leaf margin development by regulating KNOX and BEL-like transcription factors in Arabidopsis. Journal of Experimental Botany **72**, 1809–1821.

Yu Y. 2019. OsKNAT7 bridges secondary cell wall formation and cell growth regulation. Plant Physiology **181**, 385–386.

Zhan X, Zhang F, Zhong Z, Chen R, Wang Y, Chang L, Bock R, Nie B, Zhang J. 2019. Generation of virus-resistant potato plants by RNA genome targeting. Plant Biotechnology Journal **17**, 1814–1822.

Zhong R, Lee C, Zhou J, McCarthy RL, Ye ZH. 2008. A battery of transcription factors involved in the regulation of secondary cell wall biosynthesis in Arabidopsis. The Plant Cell **20**, 2763–2782.

Zipfel C, Kunze G, Chinchilla D, Caniard A, Jones JD, Boller T, Felix G. 2006. Perception of the bacterial PAMP EF-Tu by the receptor EFR restricts Agrobacterium-mediated transformation. Cell **25**, 749–760.

Zipfel C, Robatzek S, Navarro L, Oakeley EJ, Jones JD, Felix G, Boller T. 2004. Bacterial disease resistance in Arabidopsis through flagellin perception. Nature **428**, 764–767.